Journal of Applied Electrochemistry (2005) 35:733–740
DOI 10.1007/s10800-005-1381-9

Mechanism of degradation of nitrilotriacetic acid by heterogeneous photocatalysis over TiO_2 and platinized TiO_2

CARINA A. EMILIO, RAQUEL GETTAR and MARTA I. LITTER*
Unidad de Actividad Química, Centro Atómico Constituyentes, Comisión Nacional de Energía Atómica, Av. Gral. Paz 1499, 1650 San Martín, Prov. de Buenos Aires, Argentina
*(*author for correspondence, e-mail: litter@cnea.gov.ar; phone: +54-11-6 772 7016; fax: +54-11-6 772 7886)*

Received 28 June 2004; accepted in revised form 12 January 2005

Key words: heterogeneous photocatalysis, nitrilotriacetic acid (NTA), platinized TiO_2

Abstract

TiO_2-heterogeneous photocatalysis of nitrilotriacetic acid (NTA) at pH 2.5 was studied to establish the kinetic regime and the reaction mechanism. Pure Degussa P-25 and Hombikat UV100 commercial samples were compared. A Langmuirian behavior was observed over P-25. Platinization of the Hombikat sample (0.5 wt.%) caused an important increase on the photocatalytic rate with a change in the kinetics from zero order in the pure precursors to first order in the platinized sample. The nature of the intermediates and their evolution with time were compared on all systems. Glycine, iminodiacetic and oxamic acids have been identified in different proportions, together with ammonium and glycolic acid, depending on the catalyst used. The rapid depletion of NTA was not accompanied by a corresponding total organic carbon (TOC) reduction, but 84% of TOC decrease was obtained on P25 after 24 h, a very reasonable result for refractory compounds. A detailed mechanism is proposed for the photocatalytic reaction, suggested to be the same over the three catalysts here tested.

1. Introduction

Nitrilotriacetic acid (NTA) is an aminopolycarboxylic acid, extensively used as a chelating agent. In spite of being considered as a potential human carcinogen [1], it continues to be systematically employed in industrial applications [2–5]. NTA has been previously treated by different techniques including advanced oxidation technologies [3, 6–16].

Our group has been working on NTA degradation by heterogeneous photocatalysis using TiO_2, the most common photocatalyst. Preliminary results indicate that the NTA concentration, the amount of TiO_2, time and pH are important variables, and that low pHs are the most favorable [17].

On the other hand, we have also observed that although platinization of TiO_2 improves sometimes the efficiency of photocatalytic reactions, this effect depends on the substrate to be treated [18, 19]. In a recent paper, three commercial photocatalysts (Degussa P-25 (P25), Sachtleben Hombikat UV100 (HB) and Millenium PC50 (PC50)), were platinized, characterized and tested as photocatalysts in comparison with the corresponding pure samples using the degradation of EDTA and NTA as model compounds [20]. In the case of NTA, a remarkable increase in activity over the platinized samples was observed, together with a change in the kinetic regime from zero order in the pure samples to first order in Pt–TiO_2.

In the present work, we started a detailed study to elucidate the mechanism of NTA photocatalytic degradation over pure and platinized TiO_2 samples.

2. Materials and methods

2.1. *Chemicals*

TiO_2 (Degussa P-25) and Sachtleben Hombikat UV100 (HB) were commercial samples provided by the manufacturers. NTA, iminodiacetic acid (IDA), oxamic acid, glycine (Gly) were Sigma and glycolic acid and ammonium were Merck, all of the highest available purity. All other reagents were at least of reagent grade and used without further purification. Water was purified by a Nanopure system. Diluted $HClO_4$ was used for pH adjustments. A 0.5 wt.% Pt Hombikat sample (0.5HB) prepared as described previously [19], was used.

2.2. *Photocatalytic studies*

An annular glass reactor (415 mm-length, 35 mm-external diameter, 85-ml total volume) provided with a UV

lamp (Philips TLD/08, 15 W, 350–410 nm, 100% maximum transmission at 366 nm) was used for the photocalytic experiments. The total incident photon flow per unit volume, measured by ferrioxalate actinometry [21], was 4.0 μeinstein s^{-1} l^{-1} .

For the photocatalytic experiments, a fresh NTA solution (250 ml) at a known concentration was poured into a Pyrex reservoir, the catalyst (P25, HB or 0.5HB) was suspended at 1.0 g l^{-1} in the solution, and the resulting suspension ultrasonicated for 2 min. Prior to irradiation, suspensions were stirred in the dark for 30 min and the extent of adsorption was calculated by difference in the NTA concentration. The adsorbed amount was discounted to correct the initial concentration. Photocatalytic runs were done at 25 °C and the suspension was recycled at 1.0 l min^{-1} by means of a peristaltic pump. A water-saturated air stream was bubbled at 0.2 l min^{-1} in the reservoir throughout the experiment. In the case of the experiments performed to analyze the kinetic regime, pH was maintained constant at 2.5 with $HClO_4$ during the entire reaction time. In the experiments performed to analyze the intermediates, the pH was left to vary freely. Preliminary experiments showed that 2.5 was the optimal pH for the reaction. According to the values of the acid ionization NTA constants (pK_1 = 0.8, pK_2 = 1.8; pK_3 = 2.5 and pK_4 = 9.7 [22]), the predominant species in solution at pH 2.5 are the mono- and the dianion.

Samples were taken periodically from the reservoir and filtered through 0.22 μm Millipore filters for evaluation. At least, duplicated kinetic runs were carried out. Total organic carbon (TOC) was measured with a Shimadzu 5000A TOC analyzer, in the NPOC mode.

For HPLC analysis, a Konik KNK-500A liquid chromatograph with a Rheodyne Model 7125 injector and an Alltech UV–Vis detector was used, working at room temperature. NTA was determined as the Fe(III)–NTA complex [14]. The reaction intermediates generated in the photocatalytic reactions were evaluated with an anionic interchange column (Hamilton PRP X100, 250 × 4.0 mm), using 7.5 mM, pH 2.5 KH_2PO_4 as eluent, at a 1.2 ml min^{-1} flow rate and 195-nm detection. Nitrate was measured with a Wescan anion column, using 4 mM, pH 4.5 potassium biphthalate as eluent, at the same flow rate and 265-nm detection. Ammonium was analyzed as described previously [23].

3. Results and discussion

3.1. *Kinetic studies*

TiO_2 (P25) aqueous suspensions, containing NTA in concentrations ranging 0.4–6.2 mM at pH 2.5, were irradiated under near-UV light and analyzed periodically. Normalized concentration was plotted against reaction time to circumvent slight differences in concentration between experiments. The adsorption values after 30 min in the dark ranged between 5–20% depending on the initial NTA concentration. Taking into account the point of zero charge (pzc) of TiO_2 Degussa P-25 (6.5 [24]) and the pK values, NTA adsorption at pH 2.5 can be mainly attributed to electrostatic attraction.

Kinetic data were analyzed using the Langmuir–Hinshelwood model according to:

$$R_0 = \frac{kKC_0}{1 + kC_0} \tag{1}$$

where C_0 is the initial substrate concentration and R_0 is the initial photocatalytic rate, defined as the variation of the substrate concentration in the bulk vs time. k is the saturation rate and can be interpreted as the limiting rate at high solute concentrations. K is an equilibrium constant and indicates the ability of the substrate to be adsorbed or associated to the TiO_2 surface. However, it has been noted [25] that these parameters have only procedural significance and that they do not necessarily reflect interfacial phenomena.

The kinetic profiles at different NTA concentrations up to 60 min were linear in the range 2.5–6.2 mM and, at lower concentrations, they presented a deceleration after some irradiation time (not shown), typical of a Langmuir–Hinshelwood behavior. Initial rates were calculated, and a linear plot of $1/R_0$ vs $1/C_0$ was obtained (Figure 1). Kinetic constants, $k = 7.6 \times 10^{-7}$ M s^{-1} and K = 1790 M^{-1}, were similar to those obtained for other carboxylic acids submitted to similar treatments [26, 27].

3.2. *Evolution of intermediates over P25*

Experiments with 5.0 mM NTA (zero order regime) were performed for 24 h under the same conditions, except that the pH was left to vary freely. The following intermediates were identified and quantified: IDA, oxamic acid, Gly and ammonium (these names will be used for the compounds in this paper irrespective of the protolytic form due to changes in pH). The evolution and decay of the compounds are presented in Figure 2. Glycolic acid was identified but it could not be quantified due to the limit of determination of the analytical method. Some chromatograms are shown in Figure 3.

As can be observed, total NTA depletion takes place at 5 h of irradiation, following a linear decay. A stoichiometric transformation of NTA into IDA and of IDA into Gly is observed. For example, at 1 h the sum (NTA + IDA) is around the initial NTA concentration, as observed before for the homogeneous Fe–NTA/sunlight system [16]. At 8 h, when NTA has disappeared, the sum (IDA + Gly) is approximately 4.5 mM, indicating that most of the nitrogen has been transformed into these compounds. As shown, IDA and Gly formation and decomposition follow an almost linear regime, in a similar way to the decay of the parent NTA. Figure 2 also shows that oxamic acid was initially detected at 8 h, but it was produced during the whole experiment at a much lower concentration than IDA and Gly. Interestingly, there is some induction period for oxamic acid production up to 11 h, indicative that

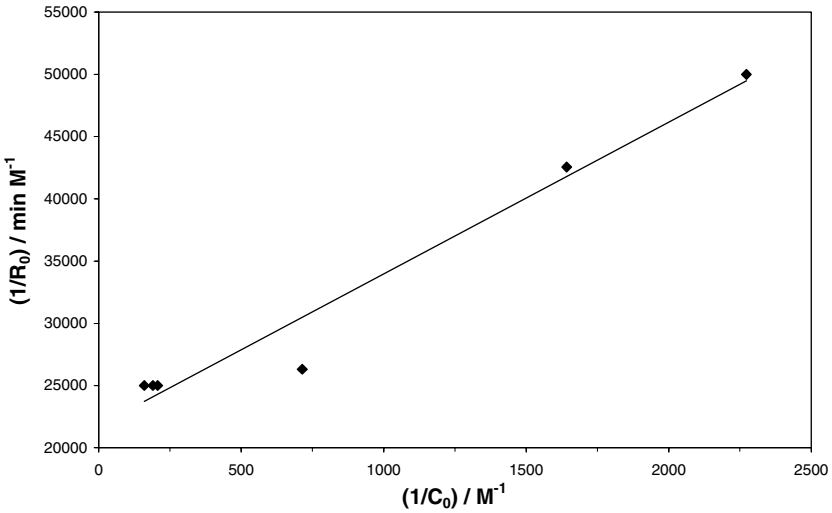

Fig. 1. Langmuirian plot for the photocatalytic degradation of NTA over P25. Conditions: pH 2.5 (fixed), TiO_2 = 1 g l^{-1}, near-UV light, P_0 = 4.0 μeinstein s^{-1} l^{-1}, oxygen bubbling at 0.2 ml min^{-1}.

IDA, Gly or some other compound is hindering its evolution. Oxamic acid formation accelerates only after total disappearance of IDA and when Gly reaches its maximum concentration (around 12 h); the maximum oxamic acid concentration (0.1 mM) is achieved around 22 h, decaying then linearly until the end of the irradiation (28 h). Ammonium was observed as traces after 4 h, increasing almost linearly since 16 h, when Gly has almost disappeared. In agreement with the formation of these basic products, pH increases slowly throughout the reaction, from 3 at 6 h up to 8 at 24 h. Then, pH decreases (e.g. 7.25 at 28 h), an evidence of volatilization of basic compounds (ammonia or amines), reinforced by the fact that, at 24 h, the sum (ammonium + oxamic) does not exceed 2.6 mM.

Nitrate was measured only at 6, 12, 18 and 24 h, but it was not detected by two possible reasons: 1) oxidation of ammonium to nitrate by holes or oxidative radicals (e.g. $HO^{\bullet}$, $O_2^{\bullet-}$is hindered by the competence of organic intermediates; 2) strong reducing species such as $CO_2^{\bullet-}$ formed from intermediates promote reduction of nitrate to ammonia [27].

Even though glyoxylic and formic acids and formaldehyde can be determined by the chromatographic method, they were not detected, because they were generated at very low concentrations, rapidly transformed to other species, volatilized by the oxygen stream or just not formed. Contrarily, our analytical method does not allow measuring oxalic acid, and other tested techniques presented interferences with some of the intermediates; this does not invalidate its formation. In contrast, minor amounts of glycolic acid could be seen from 10 to 19 h. IDA has completely disappeared at 10 h, when Gly is growing to its maximum. This suggests that glycolic acid can be formed by glycine deamination (see later).

Three non-identified peaks were also observed in the chromatograms (Figure 3), which do not correspond to acetic acid, hydroxylamine, N-methylamine, hydrazine or formamide. A deeper analysis of these unknown

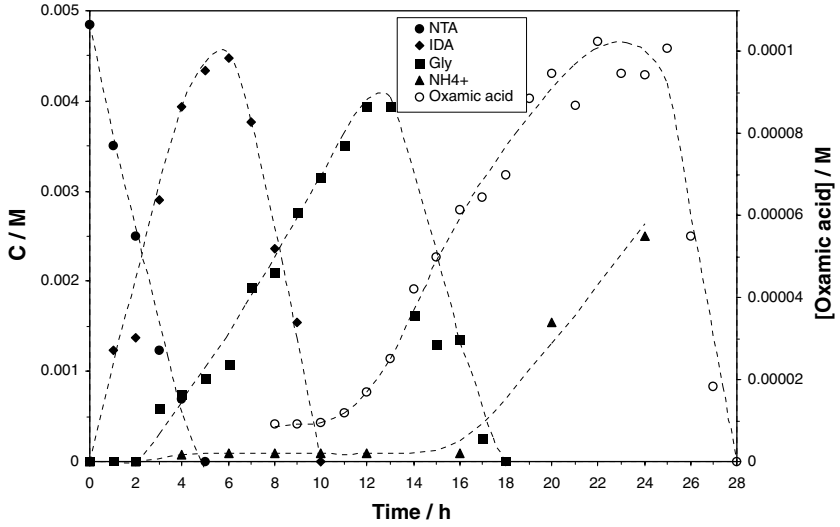

Fig. 2. Time evolution and decay of intermediates during the photocatalytic degradation of NTA over P25. Conditions as in Figure 1. pH was left to vary freely.

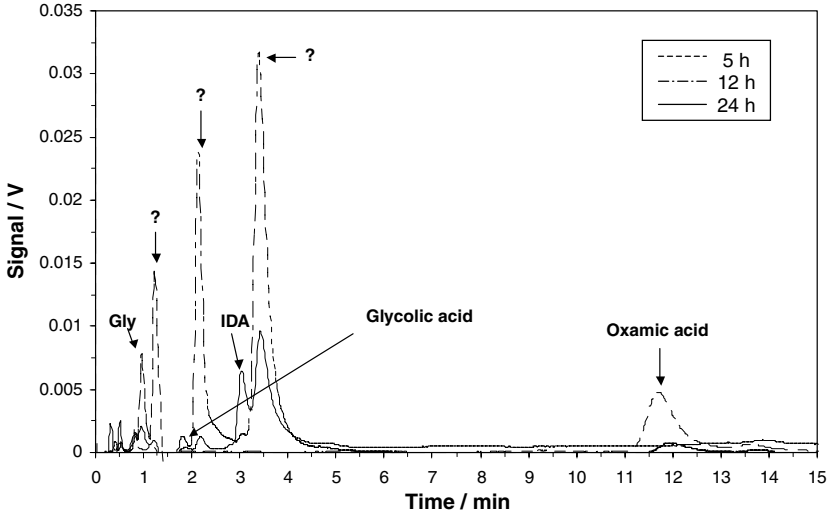

Fig. 3. Chromatograms acquired during the photocatalytic degradation of NTA over P25 at 5, 12 and 24 h of irradiation.

transients should involve the use of techniques such as HPLC-MS, to which we did not have access.

In the very well accepted heterogeneous photocatalytic mechanism, organic compounds can be oxidized directly by holes or indirectly by hydroxyl radicals ($HO^{\bullet}$), whereas conduction band electrons reduce oxygen to superoxide ($O_2^{\bullet -}$), leading to additional $HO^{\bullet}$ [28]. According to our results and those previously reported in experiments on biodegradation, γ-radiolysis and Fe–NTA photolysis [4, 5, 8, 15, 16], we propose two different points of attack on the NTA molecule: the nitrogen atom (point I) and the α-hydrogen (point II), giving rise to pathways I and II, respectively (Scheme 1). Pathway I begins by electron abstraction from the nitrogen, followed by decarboxylation:

$$R_2N{-}CH_2{-}COO^- \xrightarrow{h^+ \text{ or } HO^{\bullet}} R_2N^{\bullet +}{-}CH_2{-}COO^- \rightarrow R_2N{-}CH_2{-}COO^{\bullet} \rightarrow R_2N{-}CH_2^{\bullet} + CO_2 \quad (2)$$

where $R_2N{-}CH_2{-}COOH$ = NTA. Aliphatic free radicals react with O_2, forming peroxyl radicals that decompose to imine radicals plus superoxide [12]:

$$R_2N{-}CH_2^{\bullet} + O_2 \rightarrow R_2N{-}CH_2(O_2)^{\bullet} \rightarrow R_2N^+{=}CH_2 + O_2^{\bullet -} \quad (3)$$

Water addition to the double bond of the imine radical gives an alcohol (one of the possible non-identified products in Figure 3), which can decompose to IDA plus formaldehyde, the main products of pathway I:

$$R_2N^+{=}CH_2 + H_2O \rightarrow R_2N{-}CH_2OH \rightarrow R_2N + CH_2O \quad (4)$$

The increase in pH can be attributed also to the next reaction:

$$2O_2^{\bullet -} + 2H_2O \rightarrow 2HO^- + H_2O_2 + O_2 \quad (5)$$

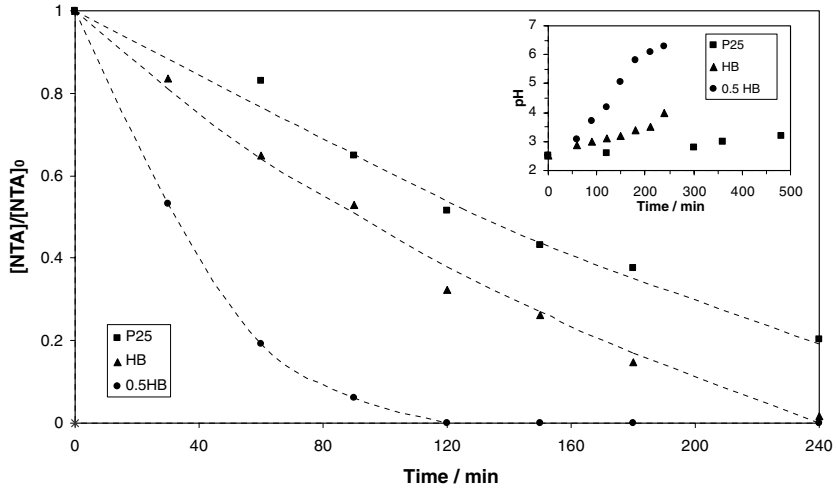

Fig. 4. Comparison of NTA evolution during the photocatalytic NTA degradation on P25, HB and 0.5HB samples. Other conditions as in Figure 1. pH was left to vary freely, as shown in the inset.

Pathway II proceeds through hydrogen abstraction from α-C-H bonds, as similarly described in γ-radiolytic experiments [12, 29]; thereby, IDA and glyoxylic acid can be formed:

$$R_2N{-}CH_2 - COOH + HO^{\bullet}(h^+) \rightarrow R_2N{-}CH^{\bullet}{-}COOH + H_2O(H^+) \quad (6)$$

$$R_2N{-}CH^{\bullet}{-}COOH + O_2 \rightarrow R_2N{-}CH^{\bullet}(O_2){-}COOH \quad (7)$$

$$R_2N{-}CH^{\bullet}(O_2){-}COOH \rightarrow R_2N^+ = CH{-}COOH + O_2^{\bullet -} \quad (8)$$

$$R_2N^+ = CH{-}COOH + H_2O\,(OH^-) \rightarrow R_2N{-}CH(OH){-}COOH \quad (9)$$

$$R_2N{-}CH(OH){-}COOH + H_2O \rightarrow R_2NH + CHO{-}COOH \quad (10)$$

Another possibility is the decay of the radical formed in (6) through (11) and/or (12), as proposed in pulse radiolysis [13, 30]:

$$2R_2N{-}CH^{\bullet}{-}COOH \rightarrow R_2N{-}\underset{\text{NTA}}{CH_2}{-}COOH + \underset{\text{IDA}}{R_2NH} + \underset{\text{Glyoxylic acid}}{CHO{-}COOH} \quad (11)$$

$$2R_2N{-}CH^{\bullet}{-}COOH \rightarrow \begin{matrix} R_2N{-}CH{-}COOH \\ | \\ R_2N{-}CH{-}COOH \end{matrix} \quad (12)$$

IDA can be decomposed also by both alternative routes, either to Gly and formaldehyde through pathway I or to Gly and glyoxylic acid through pathway II. Similarly, Gly can be transformed to ammonium and formaldehyde by route I and to glyoxylic acid and ammonium by route II.

The lack of detection of glyoxylic acid suggests that the favored route is pathway I. In our previous papers on EDTA [23, 26], glyoxylic acid was actually detected although in very low amounts (in the μM range), indicating a similar preferred route. Formaldehyde can be abundantly formed through pathway I, but as said before, it was not detected.

According to the experimental evidences, we propose the mechanism shown in Scheme 1.

Minor thermal and photochemical routes, typical of photocatalytic systems, can be also operative. For example, Gly can be oxidized to oxamic acid in a common route following I or II; oxamic acid losses ammonium and produces glyoxylic and oxalic acids, ending in CO_2. Parallelly, Gly can be deaminated to glycolic acid, as proposed for other amines and aminoacids [31]. The fact that oxamic and glycolic acids are formed in very low quantities, and that Gly is decomposed mainly to formaldehyde and ammonium by pathway I, reinforces the hypothesis that this is the main route of attack. Formic acid could be also a possible decomposition product, formed from formaldehyde or oxalic acid oxidation; however, as already said, these compounds were not found. Nevertheless, results obtained recently by us in the UV/TiO_2/oxalic acid system indicate that oxalate is degraded directly to CO_2, with no formic acid formation [32].

3.3. *Evolution of intermediates over HB and 0.5HB*

In Figure 4, experiments performed over HB and 0.5HB during 4 h of irradiation, are shown. Curve corresponding to P25 in similar conditions is added for comparison. The 0.5HB sample was chosen among other platinized samples because of its high photonic efficiency for NTA photocatalytic degradation [20]. As expected, the reactivity varies with the type of sample. For example, at 120 min, the extent of degradation follows the order P25 < HB < 0.5HB, attaining around 40, 60 and 100%, respectively. The higher activity of HB compared with P25 can be attributed to its 6-fold higher surface area [20]. A change on kinetic regime from zero to first order with 0.5HB is observed. Both results – higher activity and kinetic change – confirm our previous findings [20]. Inset of Figure 4 shows a slow pH increase with P25, somewhat faster with HB, and much higher with 0.5HB, indicating a consequently faster production of basic compounds.

An analysis of the evolution and decay of intermediates was performed to evaluate if the change on kinetic regime was due to a different degradation route with HB or 0.5 HB. In the chromatograms, no new peaks were found, indicating that either the reaction intermediates were the same formed over P25, or, if different, their detection was not possible by our chromatographic method. As before, IDA and Gly were identified in both experiments. As expected, oxamic acid was not detected on HB due to the short duration of the experiment, but it was formed on 0.5HB, although in low amounts (see later). Similarly, low amounts of glycolic acid appeared with 0.5HB at 4 h (not shown).

Figures 5 and 6 show IDA and Gly profiles. Comparison between HB and P25 shows that IDA forms initially at a similar rate, but on the first catalyst its formation levels off at 2 h and keeps constant, at least up to 4 h (Figure 5). As can be seen in Figure 6, Gly production starts on P25 after 2 h, while on HB it is produced from the beginning. This suggests that over HB some part of the produced IDA is degraded (surely to Gly, see Scheme 1), which does not occur on P25 (cf. Figures 5 and 6).

The best performance in the formation and degradation of the NTA intermediates was obtained also with 0.5HB (Figure 7). Comparison of Figures 2 and 7 indicates that the whole process occurs similarly on P25 and on 0.5HB, the latter presenting some differences: 1) a first order decay for NTA and IDA; 2) Gly production from the beginning of the reaction; 3) no induction period for oxamic acid production.

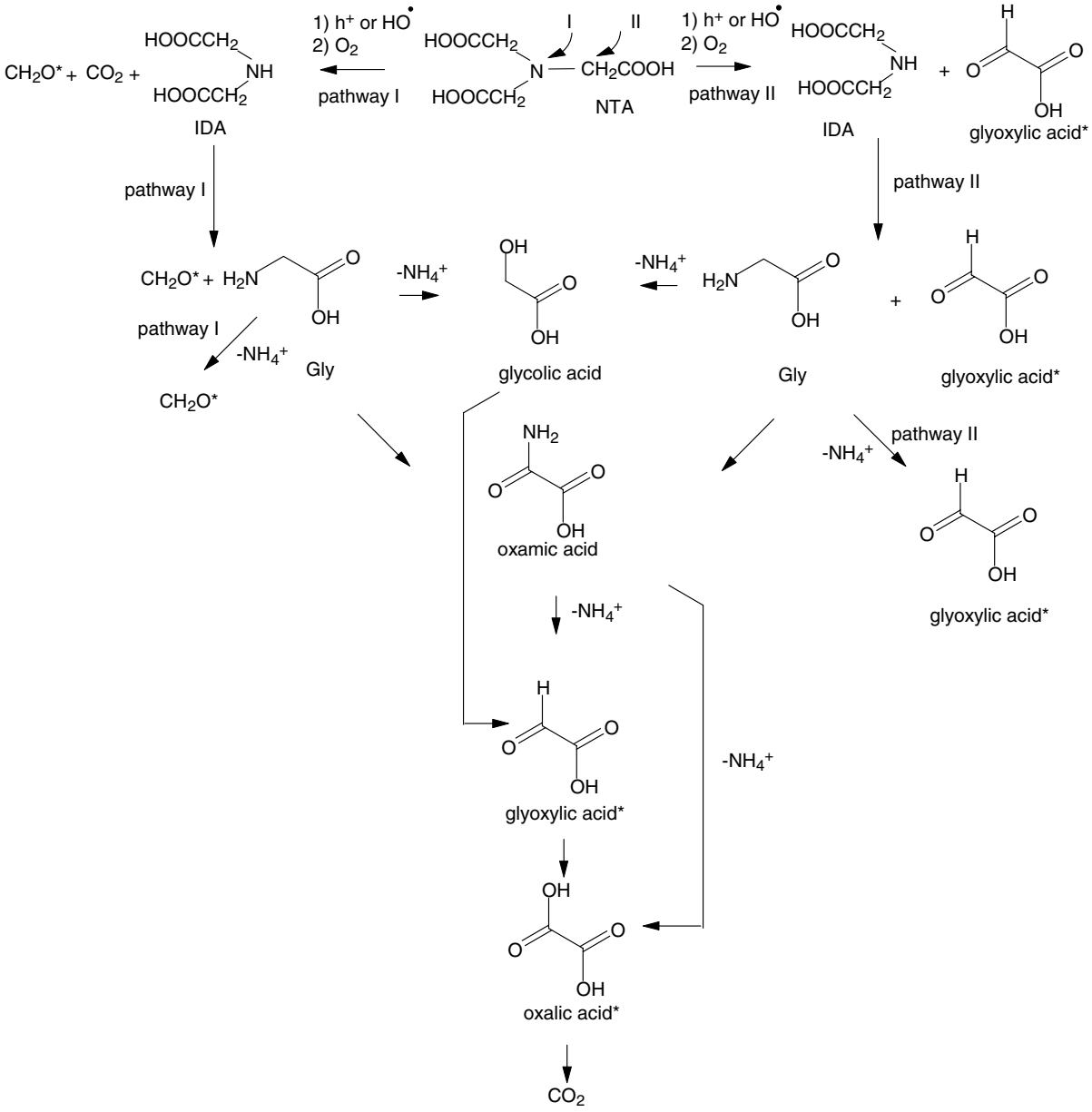

Scheme 1. Simplified possible mechanism for NTA photocatlytic degradation. *Non-detected compound.

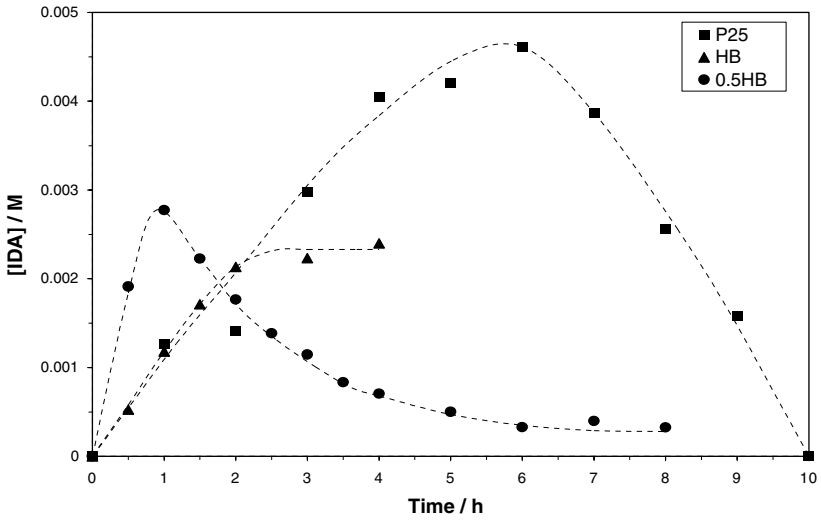

Fig. 5. Comparison of IDA evolution during the photocatalytic NTA degradation on P25, HB and 0.5HB samples. Other conditions as in Figure 1. pH was left to vary freely.

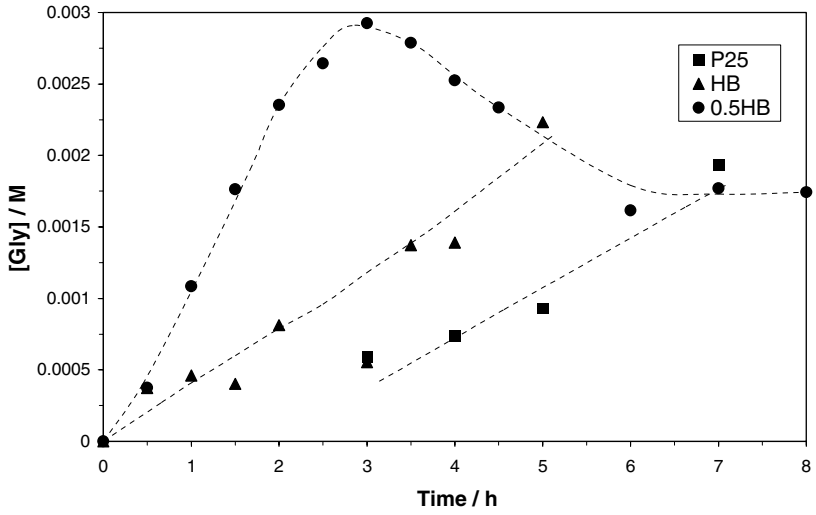

Fig. 6. Comparison of Gly evolution during the photocatalytic NTA degradation on P25, HB and 0.5HB samples. Other conditions as in Figure 1. pH was left to vary freely.

The fact that the same intermediates were formed on the three catalysts suggests a similar mechanism, proceeding predominantly through pathway I of Scheme 1. However, the time evolution of the intermediates is very dependent on the type of catalyst. As said before, a remarkable enhancement on the efficiency is obtained by platinization. Platinum islands are effective electron traps, due to the formation of a Schottky barrier at the metal–semiconductor interface, inhibiting recombination of electron and holes; platinum increases also the oxygen reduction rate (the rate determining step in most photocatalytic reactions) by decrease of the overpotential [20].

3.4. *Extent of mineralization by TOC results*

After 24 h, TOC was reduced 84% over P25, indicating a reasonable extent of mineralization for a relatively resistant compound such as NTA. Comparative TOC data obtained with the three catalysts in the first 4 h indicate that initial mineralization is very difficult, reaching similar values (30, 40 and 43% for P25, HB and 0.5HB, respectively). For technological applications, the complete absence of any harmful products at the end of the treatment must be ensured. This can be monitored by toxicity tests throughout the treatment.

4. Conclusions

A Langmuirian kinetic regime was found for the photocatalytic degradation of NTA on TiO_2 (P25) at pH 2.5. pH increases during the reaction indicating the formation of basic compounds. Major intermediates were IDA, Gly and ammonium, with minor amounts

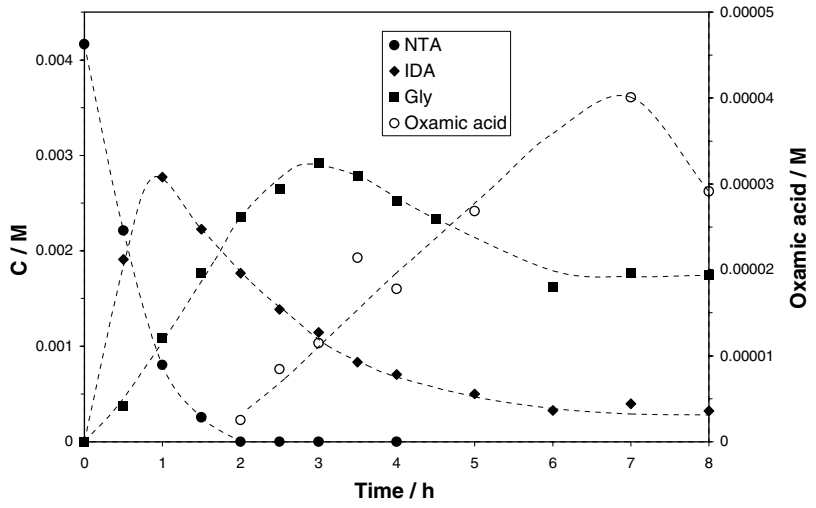

Fig. 7. Time evolution and decay of intermediates during the photocatalytic degradation of NTA over 0.5HB. Conditions as in Figure 1. pH was left to vary freely.

of oxamic and glycolic acids. A relatively good mineralization (84%) was achieved in the system after 24 h. A mechanism involving holes or $HO^{\bullet}$ attack on the organic compound and its intermediates has been proposed. From two possible mechanistic pathways, the one involving electron abstraction from the nitrogen atom of the aminocompounds is suggested to be the major route, as deduced from the nature and amount of the detected intermediates. Comparison of P25 and HB indicates that the latter is a better catalyst, due to its higher surface area. A 0.5 wt.% platinized HB was the most active sample, and a change on the kinetics from zero order in the pure precursors to first order in the platinized one was observed in both NTA and IDA degradation. However, from the identified intermediates, it is suggested that there is no change on the reaction mechanism on the three photocatalysts.

Experiments to identify other intermediates are underway, together with studies in the presence of Fe(III). The final aim of our work is to make a comparison between NTA and our previously studied EDTA system.

Acknowledgements

This work was performed as part of Comisión Nacional de Energía Atómica P5-PID-36-4 Program, Consejo Nacional de Investigaciones Científicas y Técnicas, PIP662/98 and Agencia Nacional de la Promoción de la Ciencia y la Tecnología, PICT98-13-03672. M. I. L. is a member of CONICET. C. A. E. thanks Fundación Antorchas and CNEA-CONICET for doctoral fellowships.

References

1. G.A. Crosbie, A. Lodi, J.H. McB Miller and G.G. Skellern, *J. Pharmac. Biomedical Anal.* **33** (2003) 435.
2. G. Anderegg, *Inorg. Chim. Acta* **121** (1986) 229.
3. V.E. White and C.J. Knowles, *Int. Biodeterior. Biodegrad.* **52** (2003) 143.
4. M. Sellers, Central Electricity Generating Board Report no. RD/B/N4429 (1979).
5. M. Sellers, *Radiat. Phys. Chem.* **21** (1983) 295.
6. F Muñoz and C. von Sonntag, *J. Chem. Soc., Perkin Trans.* **2** (2000) 2029.
7. R.J. Shimp, E.V. Lapsins and R.M. Ventullo, *Environ. Toxicol. Chem.* **13** (1994) 205.
8. T. Egli, *J. Bioscience Bioeng.* **92** (2001) 89.
9. A.C. Alder, H. Siegrist, W. Gujer and W. Giger, *Water Res.* **24** (1990) 733.
10. R.J. Larson, G.G. Clinckemaillie and L. Van Belle, *Water Res.* **15** (1981) 615.
11. M. Sörensen and F.H. Frimmel, *Z. Naturforsch.* **50b** (1995) 1845.
12. K. Sahul and B.K. Sharma, *J. Radioanal. Nucl. Chem.* **109** (1987) 321.
13. K. Sahul and B.K. Sharma, *Appl. Radiat. Isot.* **38** (1987) 985.
14. O. Abida, C. Emilio, N. Quici, R. Gettar, M. Litter, G. Mailhot and M. Bolte *in* A. Vogelpohl, S.U. Geißen, B. Kragert and M. Sievers (Eds.), 'Oxidation Technologies for Water and Wastewater Treatment III', *Water Sci. Technol.* **49** (2004) 123–128.
15. S.L. Andrianirinaharivelo, J.F. Pilichowski and M. Bolte, *Trans. Met. Chem.* **18** (1993) 37.
16. R.J. Stolzberg and D.N. Hume, *Environ. Sci. Technol.* **9** (1975) 654.
17. C.A. Emilio, J.F. Magallanes, M.I. Litter, The 11th International Conference on Surface and Colloid Science, Iguassu Falls, Brazil, 15–19 September 2003.
18. U. Siemon, D. Bahnemann, J.J. Testa, D. Rodríguez, N. Bruno and M.I. Litter, *J. Photochem. Photobiol. A: Chem.* **148** (2002) 247.
19. D. Hufschmidt, D. Bahnemann, J.J. Testa, C.A. Emilio and M.I. Litter, *J. Photochem. Photobiol. A: Chem.* **148** (2002) 225.
20. C.A. Emilio, J.J. Testa, D. Hufschmidt, G. Colón, J.A. Navío, D.W. Bahnemann and M.I. Litter, *J. Ind. Eng. Chem.* **10** (2004) 129.
21. C.G. Hatchard and C.A. Parker, *Proc. Roy. Soc. (London)* **A 235** (1956) 518.
22. A.E. Martell and R.M. Smith, *Critical Stability Constants*. Vol. 1 (Plenum Press, New York and London, 1974), pp. 139.
23. P.A. Babay, C.A. Emilio, R.E. Ferreyra, E.A. Gautier, R.T. Gettar and M.I. Litter, *Int. J. Photoenergy* **3** (2001) 193.
24. R. Rodríguez, M.A. Blesa and A.E. Regazzoni, *J. Colloid Interface Sci.* **177** (1996) 122.
25. E.-M. Shin, R. Senthruchelvan, J. Muñoz, S. Basak and K. Rajeshwar, *J. Electrochem. Soc.* **143** (1996) 1562.
26. P.A. Babay, C.A. Emilio, R.E. Ferreyra, E.A. Gautier, R.T. Gettar and M.I. Litter *in* A. Vogelpohl, S.U. Geissen, B. Kragert and M. Sievers (Eds.), 'Oxidation technologies for water and wastewater treatment (II)' *Water Sci. Technol.* **44** (2001) 179–185.
27. Y. Li and F. Wasgestian, *J. Photochem. Photobiol. A: Chem.* **112** (1998) 255.
28. M.I. Litter, *Appl. Catal. B: Environ.* **23** (1999) 89.
29. P. Neta, M. Simic and E. Hayon, *J. Phys. Chem.* **74** (1970) 1214.
30. J. Lati and D. Meyerstein, *J. Chem. Soc. Daltons Trans.* Vol. 1 (1978) 1105.
31. G.K.C. Low, S.R. McEvoy and R.W. Matthews, *Environ. Sci. Technol.* **25** (1991) 460.
32. N. Quici, M.E. Morgada, G. Piperata, P. Babay, R.T. Gettar and M.I. Litter, *Catal. Today*, accepted.